



Layered PLG scaffolds for *in vivo* plasmid delivery

Christopher B. Rives^a, Anne des Rieux^b, Marina Zelivyanskaya^a, Stuart R. Stock^c,
William L. Lowe, Jr.^d, Lonnie D. Shea^{a,e,*}

^a Department of Chemical and Biological Engineering, Northwestern University, 2145 Sheridan Road, Tech E136, Evanston, IL 60208, USA

^b Unité de Pharmacie de Galénique, Université Catholique de Louvain, Avenue Mounier, 73 UCL 7320, 1200 Brussels, Belgium

^c Department of Molecular Pharmacology and Biological Chemistry, Feinberg School of Medicine, Northwestern University, 303 E. Chicago Avenue, Chicago, IL 60611, USA

^d Department of Medicine, Division of Endocrinology, Metabolism and Molecular Medicine, Feinberg School of Medicine, Northwestern University, 303 E. Chicago Avenue, Tarry 15-703, Chicago, IL 60611, USA

^e The Robert H. Lurie Comprehensive Cancer Center of Northwestern University, Galter Pavilion, 675 N. Saint Clair, 21st Floor, Chicago, IL 60611, USA

ARTICLE INFO

Article history:

Received 26 June 2008

Accepted 2 September 2008

Available online 17 October 2008

Keywords:

PLG
Gene delivery
Plasmid
Angiogenesis
Scaffolds

ABSTRACT

Gene delivery from tissue engineering scaffolds can induce localized expression of tissue inductive factors to direct the function of progenitor cells, either endogenous or transplanted. In this report, we developed a layering approach for fabricating scaffolds with encapsulated plasmid, and investigated *in vivo* gene transfer following implantation into intraperitoneal fat, a widely used site for cell transplantation. Porous poly(lactide-co-glycolide) (PLG) scaffolds were fabricated using a gas foaming method, in which a non-porous layer containing plasmid was inserted between two porous polymer layers. The layered scaffold design decouples the scaffold structural requirements from its function as a drug delivery vehicle, and significantly increased the plasmid incorporation efficiency relative to scaffolds formed without layers. For multiple plasmid doses (200, 400, and 800 µg), transgene expression levels peaked during the first few days and then declined over a period of 1–2 weeks. Transfected cells were observed both in the surrounding adipose tissue and within the scaffold interior. Macrophages were identified as an abundantly transfected cell type. Scaffolds delivering plasmid encoding fibroblast growth factor-2 (FGF-2) stimulated a 40% increase in the total vascular volume fraction relative to controls at 2 weeks. Scaffold-based gene delivery systems capable of localized transgene expression provide a platform for inductive and cell transplantation approaches in regenerative medicine.

© 2008 Elsevier Ltd. All rights reserved.

1. Introduction

The fundamental goal of tissue engineering is to develop novel strategies for the replacement of diseased or injured tissues [1]. Most approaches utilize biomaterials to create a three-dimensional structure, or scaffold, that will support and guide new tissue formation from progenitor cells, either endogenous or transplanted [2,3]. Scaffolds are typically fabricated from biocompatible and biodegradable polymers, and exhibit a highly porous structure that allows for cellular infiltration and integration of the scaffold with host tissue. In cell-based therapies, scaffolds can also serve as a vehicle for delivering transplanted cells to specific sites, and must ultimately create an environment that supports cell survival and promotes their function [4]. This environment can be controlled

through localized delivery of tissue inductive factors from the scaffold to regulate key cellular events involved in tissue development or repair (e.g. differentiation, proliferation, migration) [5]. For example, the delivery of angiogenic factors from scaffolds has been widely investigated to promote new blood vessel formation [6], which is basic requirement for establishing a vascular network within the developing tissue [7]. Additionally, scaffolds can deliver factors that act directly on transplanted cells.

Gene delivery from scaffolds offers a versatile approach for manipulating soluble signals present within the local tissue microenvironment, and has the potential to provide prolonged expression of desired proteins at effective levels [8–10]. The versatility arises, in part, because plasmids have similar physical properties despite changes in the nucleic acid sequence [11], thereby allowing delivery of multiple genes with a single delivery system. Previous studies have demonstrated that plasmid delivery from both collagen and poly(lactide-co-glycolide) (PLG) scaffolds can achieve localized transfection of cells, and induce sufficient protein production to stimulate new tissue formation [12–16]. For porous PLG scaffolds, we have observed transgene expression that

* Corresponding author. Department of Chemical and Biological Engineering, Northwestern University, 2145 Sheridan Rd, Tech E136, Evanston, IL 60208, USA. Tel.: +1 847 491 7043; fax: +1 847 491 3728.

E-mail address: l-shea@northwestern.edu (L.D. Shea).

persisted for months at a subcutaneous site; however, the level and duration of transgene expression have been limited at other anatomical sites. Additionally, incorporating plasmid throughout the entire three-dimensional space of a highly porous scaffold has been relatively inefficient and dependent on the scaffold structure.

In this report, we investigated a layering approach to fabricate plasmid-releasing scaffolds that provide localized transgene expression following implantation into intraperitoneal fat, a model site for cell transplantation [17]. Porous poly(lactide-co-glycolide) (PLG) scaffolds were fabricated using a gas foaming method [14,18,19], in which a thin non-porous layer containing plasmid was inserted between two porous polymer layers. The layered scaffold design decouples the scaffold structural requirements from its function as a drug delivery vehicle. The plasmid incorporation efficiency and release rate were characterized *in vitro*, and *in vivo* transgene expression levels were measured by luciferase assay for multiple DNA doses. The distribution and identity of transfected cells were determined by immunohistochemistry. Finally, the ability of scaffolds to induce angiogenesis by providing expression of fibroblast growth factor-2 (FGF-2) was evaluated using contrast-enhanced microcomputed tomography. Scaffold-based gene delivery systems capable of localized transgene expression provide a platform for inductive and cell transplantation approaches in regenerative medicine.

2. Materials and methods

2.1. DNA sources

Plasmids were purified from bacteria culture using Qiagen reagents (Santa Clara, CA), and stored in Tris-EDTA (TE) buffer at 4 °C. All plasmids used in this study have a cytomegalovirus (CMV) promoter. The pLuc plasmid contains the firefly luciferase gene within the pNGV1 vector backbone (National Gene Vector Labs, University of Michigan). The pEGFP-C2 plasmid (CLONTECH, Palo Alto, CA) encodes green fluorescent protein. The pFGF-2 plasmid was kindly provided by Dr. Claudia Heilmann (University Hospital, Freiburg, Germany), and contains the cDNA for human fibroblast growth factor-2 (18 kDa) within the pCl-neo expression vector (Promega) [20].

2.2. Scaffold fabrication

DNA-loaded scaffolds were fabricated using a previously described gas foaming/particulate leaching process [14,18,19], with a modified scaffold design containing a non-porous center layer for DNA loading. PLG (75% D,L-lactide/25% glycolide, i.v. = 0.76 dL/g) (Lakeshore Biomaterials, Birmingham, AL) was dissolved in dichloromethane to make either a 2% (w/w) or 6% (w/w) solution, which was then emulsified in 1% poly(vinyl alcohol) to create microspheres. The scaffold outer layers were constructed by mixing 1.5 mg of 6% PLG microspheres with 50 mg of NaCl (250 $\mu\text{m} < d < 425 \mu\text{m}$) and then compressing the mixture in a 5 mm KBr die at 1500 psi using a Carver press. To make the center layer, 2 mg of 2% PLG microspheres were reconstituted in a solution containing plasmid (200, 400, or 800 μg) and lactose (1 mg), and then lyophilized. This lyophilized product was then sandwiched between two outer layers and compressed at 200 psi. The composite scaffold was then equilibrated with high pressure CO₂ gas (800 psi) for 16 h in a custom-made pressure vessel. Afterwards, the pressure was released over a period of 25 min, which serves to fuse adjacent microspheres creating a continuous polymer structure. To remove the salt, each scaffold was leached in 4 mL of water for 2.5 h while shaking at 110 rpm, with fresh water replacement after 2 h.

2.3. Scanning electron microscopy (SEM)

Structural characteristics of scaffolds were imaged with a scanning electron microscope (Hitachi S-3400N-II) using the variable pressure mode and an ESED detector. The microscope was operated at an electron voltage of 15 kV.

2.4. DNA incorporation and *in vitro* release

The incorporation efficiency and *in vitro* release were determined as a function of DNA loading. The DNA incorporation efficiency is defined as the mass of DNA left in the scaffold after the leaching step divided by the mass of DNA initially inputted. Hereafter, the amount of input DNA will be referred to as the dose. Scaffolds were loaded with 200, 400, or 800 μg of pLuc. After leaching, scaffolds were dissolved in chloroform (600 μL), and the DNA was extracted from the organic solution. TE Buffer (400 μL) was added to the organic phase, vortexed, and centrifuged at 14,000 rpm for 3 min. The aqueous layer was collected, and two more extraction cycles were performed to maximize DNA recovery. The amount of DNA was

quantified using a fluorometer and the fluorescent dye Hoechst 33258. To determine the *in vitro* release kinetics of DNA, scaffolds were placed in 500 μL of phosphate-buffered saline (PBS) (pH 7.4) at 37 °C, and the solution was replaced at each time-point. The conformation of the released DNA was analyzed by agarose gel electrophoresis. A digital image of the gel was taken and NIH image software was used to evaluate the fraction of DNA remaining in the supercoiled conformation as previously described [21].

2.5. Measuring *in vivo* transgene expression

Animal studies were performed in accordance with the NIH Guide for the Care and Use of Laboratory Animals, and protocols were approved by the IACUC at Northwestern University. Scaffolds loaded with luciferase-encoding plasmid (200, 400, or 800 μg) were sterilized in 70% ethanol, washed in RPMI-1640 growth medium (Gibco-BRL, Grand Island, NY) (supplemented with 10% heat inactivated fetal calf serum (Hyclone, Logan, UT), 100 U/mL penicillin-G, 100 mg/mL streptomycin sulfate, and 1 mmol/L L-glutamine) to mimic the cell transplantation procedure, and then implanted into intraperitoneal fat of 10–12 week old C57BL/6 male mice (Jackson Laboratories), as previously described [17]. The selection of plasmid doses was based on previous reports [14–16]. At 3, 7, 14, and 21 days post-implantation, scaffolds were retrieved and frozen over dry ice. The frozen tissue samples were cut into small pieces with scissors, immersed in 200 μL of cell culture lysis reagent (Promega), and placed on a rotator for 30 min. Then samples were snap frozen in liquid nitrogen, thawed in a 37 °C water bath, and centrifuged at 14,000 rpm for 10 min at 4 °C. The supernatant was mixed with luciferase assay reagent (Promega) and luciferase activity was measured with a luminometer using a 10 s integration time. Samples were normalized by total protein amount, which was measured using a BCA protein assay (Pierce Biotechnology Inc., Rockford, IL).

2.6. Histological analysis and immunohistochemistry

Histological analysis was performed to determine the cellular distribution and identity of transfected cells. Scaffolds loaded with 400 or 800 μg of GFP plasmid were retrieved 7 and 14 days post-implantation and frozen in an isopentane bath cooled over dry ice. Tissue samples were embedded in Tissue-Tek O.C.T. compound (Sakura Finetek, Torrance, CA) and sections were cut at 14 μm thickness using a cryostat. Prior to staining, sections were fixed with 4% paraformaldehyde for 10 min and washed in PBS. The extent of cellular infiltration into scaffolds was visualized by hematoxylin and eosin (H&E) staining of tissue sections at 7 and 14 days. The distribution of transfected cells was determined by performing immunohistochemistry using an antibody directed against green fluorescent protein (GFP). Additionally, an antibody directed against the macrophage surface marker, F4/80, was used to determine if the cell type transfected was macrophages. After blocking, the two primary antibodies (rabbit anti-GFP (1:500 dilution; Invitrogen) and rat anti-mouse F4/80 (1:100 dilution; AbD Serotec, Raleigh, NC)) were applied for 2 h at room temperature. Secondary antibodies (Alexa Fluor 546 nm goat anti-rat (1:500 dilution; Invitrogen) and Alexa Fluor 488 nm goat anti-rabbit (1:500 dilution; Invitrogen)) were used to visualize the antigens. Lastly, sections were incubated with Hoechst 33258 (Invitrogen) (10 mg/mL, 1:2000 dilution) for 5 min to allow visualization of cell nuclei.

2.7. Evaluation of angiogenesis using microcomputed tomography

A previously described method for contrast-enhanced microcomputed tomography was used to evaluate blood vessel formation in scaffolds delivering plasmid encoding an angiogenic factor [22]. Scaffolds were loaded with 800 μg of pFGF-2 or 800 μg of pGFP and implanted into mice as described above. Control scaffolds were loaded with pGFP, rather than no DNA, to separate any effects of plasmid delivery from the response due to expression of FGF-2. At 2 weeks post-implantation, animals were deeply anesthetized by an intraperitoneal injection of tribromoethanol and placed ventral side up on a perfusion tray. The thoracic cavity was opened and a 21-gauge needle was inserted into the left ventricle and secured in place. The right atrium was cut and a peristaltic pump was used to flush the vasculature with 25 mL of normal saline containing heparin sodium (10 U/mL) at a rate of ~5 mL/min. The specimen was then fixed by perfusion with 75 mL of 4% paraformaldehyde. The fixative was subsequently flushed from the vasculature with heparinized saline. A radiopaque silicone rubber compound containing lead chromate (Microfil MV-122, Flow Tech Inc., Carver, MA) was mixed with a curing agent, and then manually injected into the vasculature. Specimens were stored at 4 °C overnight to allow for polymerization of the compound, and then tissue samples were surgically retrieved. Samples were stored in 4% paraformaldehyde at 4 °C until imaging.

Samples were imaged using a Scanco Micro-CT 40 system (Basserdorf, Switzerland) operated at a voltage of 45 kV and current of 88 μA . Samples were scanned in a 16.4 mm diameter sample holder at high resolution, creating a series of 2048 \times 2048 voxel (volume element) reconstructed slices with isotropic voxel size of ~8 μm . Each scan consisted of 160 slices through the center of the sample. Reconstructed serial slices were globally thresholded based on X-ray attenuation and used to create 3-D renderings of the vascular networks. The same threshold (200 on a scale from 0 to 1000, corresponding to linear attenuation coefficients from 0 to 8 cm^{-1} ,

respectively) was used for all samples. The vascular volume fraction was calculated directly from the 3-D renderings, based on the voxel size and the number of segmented voxels in the 3-D image. The distribution of vessel diameters was calculated using a model-independent method for assessing thickness in 3-D images [23].

2.8. Statistical analysis

Values are reported as the mean \pm standard deviation. Statistical calculations were performed using JMP 4.0.4 software (SAS Institute, Cary, NC), and *P* values were determined by a *t*-test.

3. Results

3.1. Layered scaffold design

A layered scaffold design was developed to facilitate the efficient incorporation of large quantities of plasmid, while retaining a well-interconnected open-pore structure suitable for cell transplantation. The design consists of a thin, non-porous center layer that is sandwiched between two highly porous outer layers (Fig. 1A–C). The composite scaffold is formed by fusion of microspheres during the gas foaming process, resulting in an effective union between adjacent layers. The center layer can be used for plasmid delivery, while the outer layers provide a platform for cell-seeding and support tissue infiltration. By constructing a scaffold with different layers, the design requirements for the physical structure (i.e. outer layers) were decoupled from the delivery system (i.e. center layer).

3.2. DNA incorporation and in vitro release

The layered scaffold design substantially improved DNA incorporation efficiency relative to previous reports of scaffolds made with the gas foaming/particulate leaching process [14,15]. The incorporation efficiencies for 200 and 400 μg of DNA were $76.8 \pm 4.9\%$ and $75.7 \pm 4.5\%$, respectively (Table 1). For 800 μg of DNA, the incorporation efficiency was further increased to $86.8 \pm 6.3\%$ (Table 1), which was significantly higher than the other two doses ($P < 0.05$).

In characterizing DNA release, a large initial burst was observed within the first 3 days, although the magnitude of the burst increased with increasing dose (Fig. 2A). The initial bursts were equal to $73.3 \pm 2.4\%$, $83.6 \pm 1\%$, and $89.9 \pm 2.5\%$ for the 200, 400, and 800 μg doses, respectively (Fig. 2A). The rapid release of plasmid may reflect release caused by the porosity of the center layer, which results from the sugars used as cryoprotectants and the DNA itself. Rhodamine labeling of plasmid has indicated a thorough distribution of plasmid throughout the center layer (data not shown). For all three doses, a similar amount of DNA ($\sim 30 \mu\text{g}$) remained trapped in the scaffolds and was not released, indicating that some plasmid may be more deeply embedded within the center layer. Notably, as the dose decreases, 30 μg becomes a larger percentage of the total amount of incorporated DNA, causing a shift in the release curves. Following the initial burst, a sustained DNA

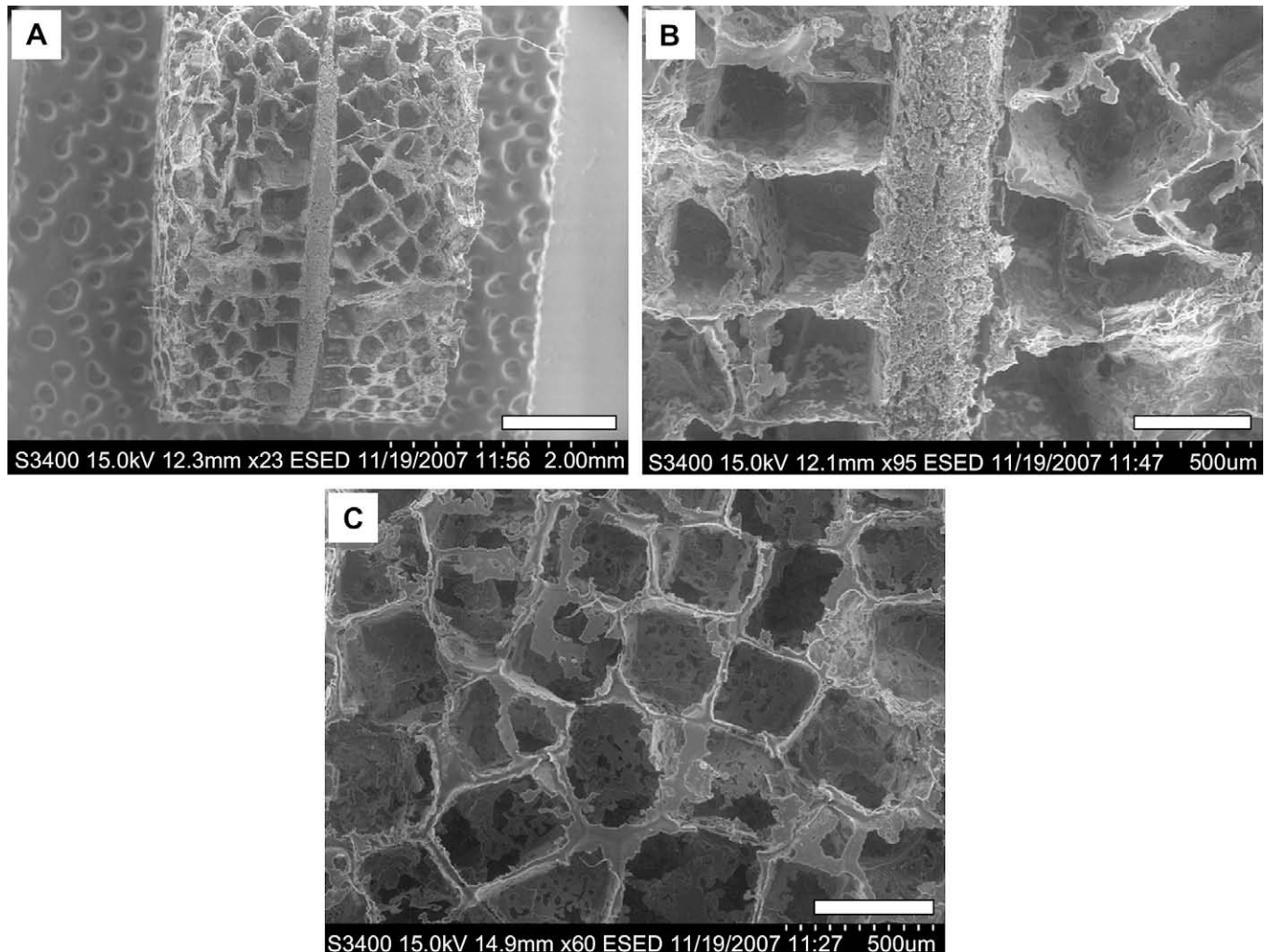


Fig. 1. Scanning electron micrographs of a layered PLG scaffold. (A) Side view of the composite scaffold. Scale bar equals 1 mm. (B) Magnified view of the center layer. Scale bar equals 250 μm . (C) Magnified view of the pore structure in the outer layer. Scale bar equals 400 μm .

Table 1
DNA incorporation efficiency

Input DNA (μg)	Incorporated DNA (μg)	Incorporation efficiency (%)
200	153.7 \pm 9.8	76.8 \pm 4.9
400	302.7 \pm 17.8	75.7 \pm 4.5
800	694.5 \pm 50.1	86.8 \pm 6.3

release was observed for up to 2 weeks (Fig. 2A). Overall, the DNA release profiles obtained here are similar to previous reports [14,15]. Increasing the mass of polymer contained in the center layer above 2 mg (up to 5 mg) did not further improve the incorporation efficiency or slow the release rate (data not shown). Analysis by agarose gel electrophoresis confirmed that a large proportion of released DNA remains in the supercoiled conformation, although there is a gradual increase in the conversion to nicked and linear conformations over time (Fig. 2B, Table 2). This decrease in supercoiled conformation is consistent with previous reports of plasmid release from PLG microspheres and scaffolds, and the nicked conformation has been shown to have similar transfection competence relative to supercoiled [14,15,24]. The mechanism responsible for plasmid nicking is proposed to be a combination of polymer processing and polymer degradation [24,25].

3.3. In vivo transgene expression

The ability of DNA-releasing scaffolds to promote *in vivo* gene transfer at the intraperitoneal fat site was evaluated for multiple DNA doses. For all doses tested (200, 400, and 800 μg), transgene

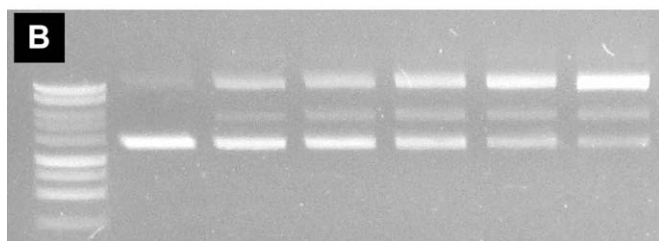
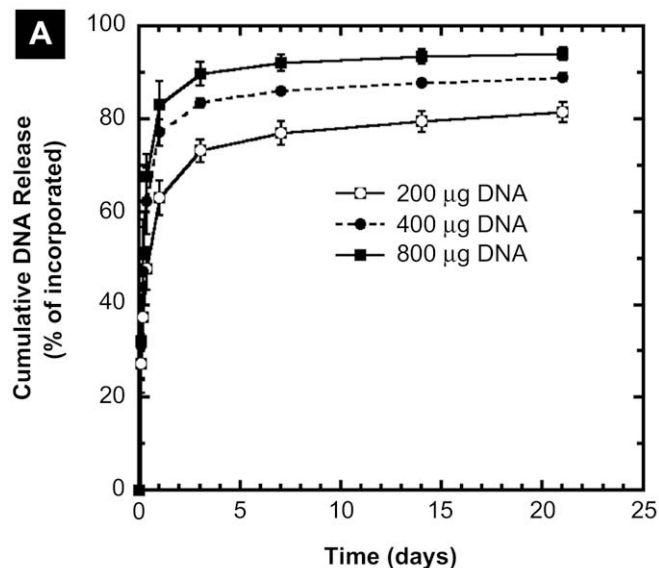


Fig. 2. *In vitro* DNA release kinetics and agarose gel electrophoresis. (A) Cumulative DNA release from scaffolds loaded with 200, 400, or 800 μg of plasmid ($n = 4$ per dose) (B) Image of an agarose gel containing DNA released from a scaffold at different times. Lane 1: molecular weight marker. Lane 2: unincorporated plasmid. Lanes 3–7: DNA released at days 1, 3, 7, 14, and 21, respectively.

Table 2
Conformational analysis of plasmid release from scaffolds

Lane	Sample	Nicked (%)	Linear (%)	Supercoiled (%)
1	Molecular weight marker	–	–	–
2	Unincorporated DNA	14.7	0.0	85.3
3	DNA released between 8 and 24 h	36.3	10.3	53.5
4	DNA released between 1 and 3 days	38.2	14.4	47.4
5	DNA released between 3 and 7 days	45.8	16.1	38.2
6	DNA released between 7 and 14 days	53.9	16.9	29.2
7	DNA released between 14 and 21 days	61.8	17.1	21.1

expression levels peaked during the first few days and declined substantially over a period of 1–2 weeks (Fig. 3). Transgene expression decreased to background levels in most animals by 21 days (data not shown). The DNA dose had little effect on transgene expression levels at day 3, as all doses achieved similarly robust expression levels (Fig. 3). This result indicates that the amount of DNA initially released was not a limiting factor in gene transfer for any of the doses tested (Fig. 3). However, at days 7 and 14, the 400 and 800 μg doses resulted in higher levels of transgene expression relative to the 200 μg dose (Fig. 3). The higher doses provide greater absolute quantities of plasmid release, which may lead to increased local DNA concentrations for longer times and thus enhanced gene transfer. Interestingly, the 400 and 800 μg doses achieved similar expression levels at all time-points, suggesting a threshold above which further increases in dose do not increase expression (Fig. 3). The rapid plasmid release observed here may limit the extent to which higher expression levels can be achieved through increases in dose.

3.4. Histological analysis and immunohistochemistry

The layered scaffolds maintained structural integrity and the outer porous regions effectively supported cellular infiltration, as indicated by H&E staining at days 7 and 14 (Fig. 4A and B). Immunohistochemical staining was performed to determine the distribution and identity of transfected cells. Scaffolds loaded with 400 or 800 μg of GFP-encoding plasmid were retrieved at 7 and 14 days, and stained with an antibody directed against GFP (transgene product) and F4/80 (macrophage surface marker). Staining results were similar for both doses and time-points. It is important

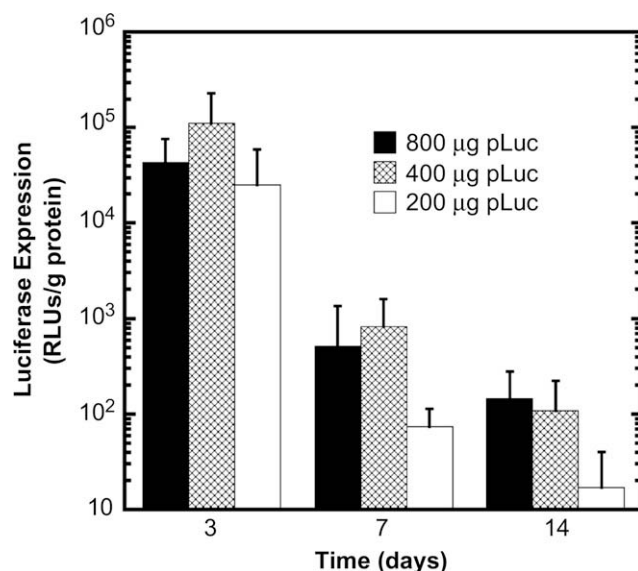


Fig. 3. *In vivo* luciferase transgene expression for scaffolds loaded with 200, 400, or 800 μg of pLuc ($n = 4$ per dose per time-point).

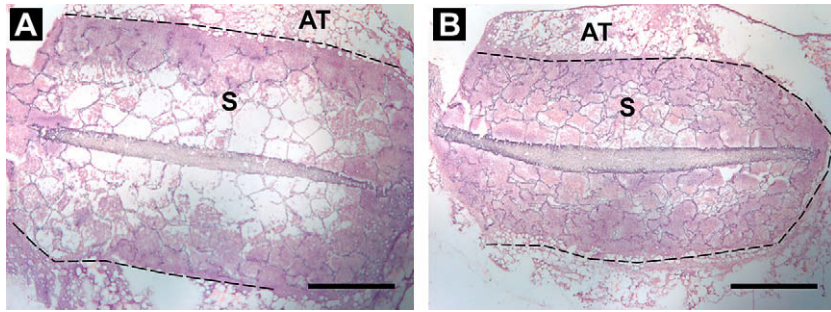


Fig. 4. H&E staining of cellular infiltration into outer layers of scaffold. Scaffold cross-section at (A) day 7 and (B) day 14. 25x magnification, scale bars equal 1 mm. S indicates scaffold region, AT indicates surrounding adipose tissue, and the dashed line indicates the interface.

to note that preadipocytes (i.e. adipocyte precursors) and macrophages share numerous functional and antigenic properties, and that preadipocytes can rapidly convert into macrophages [26]. Thus, macrophage presence at this site likely arises from both macrophage recruitment and conversion of resident preadipocytes into macrophages. Low magnification images taken at the interface of the scaffold with surrounding adipose tissue demonstrate the presence of GFP⁺ transfected cells (green) and macrophages (red) in both regions (Fig. 5A–C). Higher magnification images focusing on the surrounding adipose tissue clearly indicate co-localization of GFP and F4/80 staining (yellow), revealing that a large number of the transfected cells are macrophages (Fig. 5D–F). Similarly, higher magnification images focusing on a region within the scaffold show co-localization of GFP and F4/80 staining

immediately adjacent to the polymer (Fig. 5G–I). The presence of transfected cells immediately adjacent to the polymer surface has been observed previously [15], although here we have identified them as macrophages.

3.5. Angiogenesis

Scaffolds releasing plasmid encoding the angiogenic factor, FGF-2, were evaluated for their ability to induce new blood vessel formation. Angiogenesis is a critical component of cell transplantation approaches, where the establishment of a sufficient vascular supply is required to support cell survival. Given both the need to rapidly induce blood vessel formation and the observed duration of transgene expression, vascular growth was evaluated at

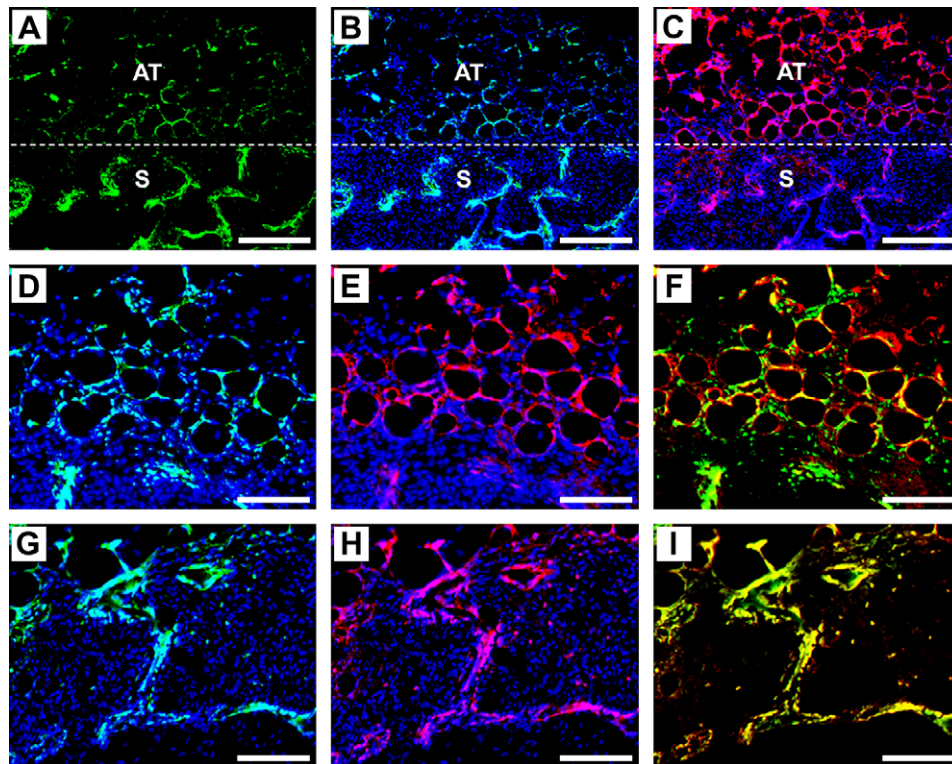


Fig. 5. Immunohistochemical staining to determine the distribution and identity of transfected cells. Images were taken from a scaffold loaded with 400 μ g of GFP plasmid that was retrieved after 7 days. For (A–C), 100 \times magnification images were captured at the interface of the scaffold with surrounding adipose tissue (scale bars equal 200 μ m). (A) GFP antibody staining. (B) GFP antibody staining with Hoechst staining for cell nuclei. (C) F4/80 (macrophage) antibody staining with Hoechst. “S” indicates scaffold region, “AT” indicates adipose tissue, and dashed line indicates interface. For (D–F), 200 \times magnification images were captured in adipose tissue outside scaffold (scale bars equal 100 μ m). (D) GFP antibody staining with Hoechst. (E) F4/80 antibody staining with Hoechst. (F) GFP antibody and F4/80 antibody staining. Yellow indicates co-localization of GFP and F4/80, and thus transfected macrophages. For (G–I), 200 \times magnification images were captured within the scaffold (scale bars equal 100 μ m). (G) GFP antibody staining with Hoechst. (H) F4/80 antibody staining with Hoechst. (I) GFP and F4/80 antibody staining. [For interpretation of the references to colour in this figure legend, the reader is referred to the web version of this article.]

2 weeks. Scaffolds releasing pFGF-2 provided a 40% increase in the total vascular volume fraction relative to controls ($P < 0.01$, Fig. 6A). This increase in vascularization was also apparent in the 3-D renderings of the vascular networks (Fig. 6B and C). A histogram showing the distribution of vessel diameters demonstrates a significant increase in the presence of larger vessels ($>200 \mu\text{m}$) for the FGF-2 scaffolds relative to controls ($P < 0.05$, Fig. 6D). This result indicates that the increase in vascular volume fraction for FGF-2 scaffolds was partly due to an increase in vessel size. FGF-2 has been reported to increase the size of vessels in addition to promoting the sprouting of new vessels [20].

4. Discussion

This report describes a layering approach for scaffold fabrication that utilizes a thin, non-porous central layer to facilitate efficient incorporation of large quantities of plasmid. The underlying premise of this approach is that the physical properties of a scaffold (e.g. porosity, degradation rate) best suited for tissue growth may not be optimal from a drug delivery perspective, thereby creating critical design constraints. By implementing a layered design, the scaffold structural requirements can be decoupled from its function as a drug delivery vehicle. In the context of the current study, we were faced with the challenge that incorporating DNA throughout the entire three-dimensional space of a highly porous polymer scaffold is associated with large losses of DNA during the particulate leaching step. By confining the DNA within a non-porous layer in the center of the scaffold, the incorporation efficiency was substantially increased. The porosity of the center layer directly

influenced the DNA incorporation efficiency, as incorporation increased with decreasing porosity. The scaffold symmetry (i.e. porous layers on both sides of the center layer) may also contribute to the increased DNA incorporation by minimizing exposure of the center layer to water during the particulate leaching step. Additionally, the symmetry provides an opportunity for cell transplantation on both sides of the scaffold. The layered scaffold design can also be employed for the controlled delivery of proteins. Proteins can be encapsulated within polymer microspheres, and the protein-loaded microspheres can be used to construct the center layer of the scaffold. An important advantage of this novel approach to scaffold fabrication is that the layered design affords more flexibility in choosing a polymer formulation (e.g. M_w , lactide:glycolide ratio) that provides appropriate release kinetics, since the structural requirements of the outer layers will not be affected by the properties of the center layer.

The broader applicability of this layered scaffold design will likely depend upon the materials, processing methods, and applications. The layering strategy is readily amendable to the gas foaming process employed here, since each layer can be formed separately and then subsequently fused together. Other amorphous polymers in addition to PLG may potentially be processed by gas foaming, and other strategies for fusing polymers may be possible (e.g. melt fusion) [27,28] as long as the integrity of the plasmid is not impacted. For the layered PLG scaffold described here, the mechanical properties of the scaffold are limited by the porous outer layer, and thus applications requiring significant load bearing (e.g. bone) may not be appropriate. Ceramic materials can provide mechanical properties compatible with load bearing applications

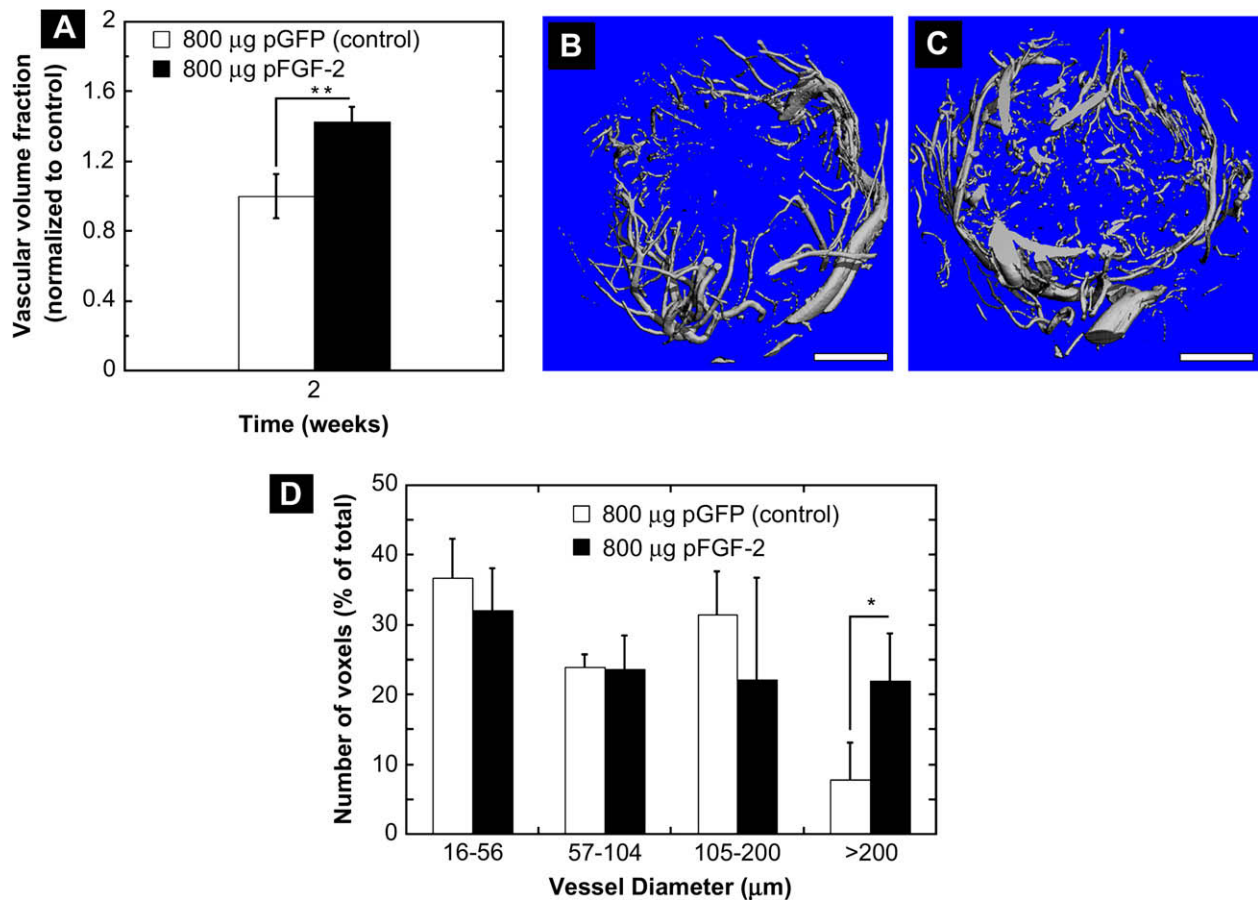


Fig. 6. Microcomputed tomography analysis of angiogenesis at 2 weeks. (A) Total vascular volume fraction for scaffolds releasing FGF-2 plasmid or GFP plasmid (control) ($n = 3$ per condition). $**P < 0.01$. 3-D renderings of vascular networks formed in (B) a control scaffold and (C) an FGF-2 scaffold. Scale bars equal 1 mm. (D) Histogram showing the distribution of vessel diameters for FGF-2 and control scaffolds. $*P < 0.05$.

and have been processed by sintering to create porous scaffolds [29]. However, the temperatures employed to sinter hydroxyapatite may reduce the plasmid integrity. Layering strategies have also been employed for crosslinked hydrogels and may be effective in creating defined regions with varied functionalities [30].

The kinetics of *in vivo* transgene expression obtained here with the layered scaffold may result from the release profile and the plasmid design. The plasmid release likely provides ample quantities of plasmid initially, yet insufficient quantities of plasmid at later times. A more sustained release profile may extend transgene expression by maintaining higher concentrations of the vector over time, thereby allowing for continued cellular transfection. Alternative methods of slowing plasmid release are possible, such as microsphere encapsulation prior to scaffold formation [16,24,31], which could be merged with the layering strategy. Decreasing the burst of plasmid may also reduce the inflammatory response, as large quantities of bacterially derived plasmid activate inflammatory cells due to the presence of unmethylated CpG sequences. These CpG motifs can also lead to silencing of the promoter, which has been particularly noted for the CMV promoter [32]. Alternative mechanisms that limit transgene expression include cytokine-mediated inhibition [33], binding of repressor proteins [34], methylation [35], or loss of a positive activator [36]. In some cases, the use of alternative promoters has allowed for more sustained gene expression [32]. Additionally, modification of the plasmid vector through depletion of CpG motifs can prolong transgene expression [37,38].

A large number of transfected cells at the intraperitoneal fat site were identified as macrophages using immunohistochemistry. Previous studies investigating plasmid delivery at other sites have typically implicated either fibroblasts or endothelial cells as the primary cell types responsible for expressing the plasmid [13,16]. The transfection of macrophages has been reported to involve a specific transport mechanism for the uptake of plasmid, involving scavenger-like receptors that recognize a variety of anionic macromolecules [39,40]. Although much of the internalized DNA is degraded in endosomal compartments, some plasmid remains intact for nuclear transport, especially when delivered at high concentrations [41]. Plasmid delivery from a polymer-coated stent produced *in vivo* transfection of macrophages at 7 days after implantation [42]. Efficient *ex vivo* transfection of primary macrophages has also been demonstrated using gelatin particles complexed with plasmid [43]. An important implication for the transfection of macrophages is their potential to provide long-term transgene expression, since they are essentially non-dividing and have life spans up to several months [44]. Also, macrophages are part of the normal inflammatory response following implantation of a biomaterial, and will be present regardless of the implant site. Thus, macrophages represent a widely applicable target for gene transfer. However, the intensity and duration of the inflammatory response may be related to the transfection profile obtained. While the transfection of macrophages likely relies on their specific mechanism for internalizing plasmid, other strategies may be employed to potentially target different cell types. For example, plasmid can be complexed with a transfection reagent that would serve to provide a mechanism to facilitate internalization and cellular trafficking in cell types other than macrophages. Alternatively, these vectors can be designed with ligands to facilitate binding to specific cell types [45]. The layered scaffold design provides a general approach for controlling release of encapsulated factors, and may be broadly applicable to these other gene delivery strategies.

The presence of transfected cells adjacent to the polymer surfaces within scaffolds has been observed in prior reports, although the current results provide new insight for the interpretation of this observation. Cellular transfection preferentially

near the polymer was previously hypothesized to result from the polymer surface having the highest DNA concentrations [15], as DNA was encapsulated throughout the scaffold structure. However, in these layered scaffolds, plasmid was loaded only in the center layer, and transfected cells were found throughout the porous polymer region and in the adjacent tissue. Thus, transfection in these outer, porous regions is likely not related simply to high DNA concentrations. Rather, the identification of macrophages as the predominant cell type transfected, and the propensity of macrophages to associate with biomaterial surfaces [46], together may explain this observation of transfected cells near the polymer surface.

5. Conclusions

A layered scaffold design was developed to facilitate the efficient incorporation of large quantities of plasmid, while maintaining a suitable physical structure for cell transplantation. DNA-releasing scaffolds promoted *in vivo* gene transfer at an intraperitoneal fat site, with transgene expression persisting for up to 2 weeks. Regardless of the plasmid dose, a similar trend was observed where expression levels peaked during the first few days and then rapidly declined. Immunohistochemical analysis demonstrated abundant transfected cells both in the surrounding tissue and within the scaffold pores. A large number of these transfected cells were identified as macrophages. Scaffolds delivering plasmid encoding the angiogenic factor, FGF-2, significantly increased the extent of blood vessel formation relative to controls. Understanding the requirements for maximizing the extent and duration of transgene expression remains a challenge for the successful design and implementation of scaffold-based gene delivery systems. The continued development of this approach will likely enhance the efficacy of cell-based therapies for a variety of applications.

Acknowledgements

The authors would like to thank Hannah Tuinstra for assistance with scanning electron microscopy and Laura De Laporte for helpful discussions. Financial support for this research was provided by NIH EB003806.

Appendix

Figures with essential colour discrimination. Certain figures in this article, particularly Figs. 4 and 5, are difficult to interpret in black and white. The full colour images can be found in the on-line version, at doi:10.1016/j.biomaterials.2008.09.013.

References

- [1] Langer R, Vacanti JP. Tissue engineering. *Science* 1993;260(5110):920–6.
- [2] Putnam AJ, Mooney DJ. Tissue engineering using synthetic extracellular matrices. *Nat Med* 1996;2(7):824–6.
- [3] Kim BS, Mooney DJ. Development of biocompatible synthetic extracellular matrices for tissue engineering. *Trends Biotechnol* 1998;16(5):224–30.
- [4] Mooney DJ, Vandenburgh H. Cell delivery mechanisms for tissue repair. *Cell Stem Cell* 2008;2(3):205–13.
- [5] Hill E, Boonthekul T, Mooney DJ. Regulating activation of transplanted cells controls tissue regeneration. *Proc Natl Acad Sci U S A* 2006;103(8):2494–9.
- [6] Zisch AH, Lutolf MP, Hubbell JA. Biopolymeric delivery matrices for angiogenic growth factors. *Cardiovasc Pathol* 2003;12(6):295–310.
- [7] Patel ZS, Mikos AG. Angiogenesis with biomaterial-based drug- and cell-delivery systems. *J Biomater Sci Polym Ed* 2004;15(6):701–26.
- [8] Jang JH, Houchin TL, Shea LD. Gene delivery from polymer scaffolds for tissue engineering. *Expert Rev Med Devices* 2004;1(1):127–38.
- [9] Storrer H, Mooney DJ. Sustained delivery of plasmid DNA from polymeric scaffolds for tissue engineering. *Adv Drug Deliv Rev* 2006;58(4):500–14.
- [10] De Laporte L, Shea LD. Matrices and scaffolds for DNA delivery in tissue engineering. *Adv Drug Deliv Rev* 2007;59(4–5):292–307.
- [11] Middaugh CR, Evans RK, Montgomery DL, Casimiro DR. Analysis of plasmid DNA from a pharmaceutical perspective. *J Pharm Sci* 1998;87(2):130–46.

- [12] Fang J, Zhu YY, Smiley E, Bonadio J, Rouleau JP, Goldstein SA, et al. Stimulation of new bone formation by direct transfer of osteogenic plasmid genes. *Proc Natl Acad Sci U S A* 1996;93(12):5753–8.
- [13] Bonadio J, Smiley E, Patil P, Goldstein S. Localized, direct plasmid gene delivery *in vivo*: prolonged therapy results in reproducible tissue regeneration. *Nat Med* 1999;5(7):753–9.
- [14] Shea LD, Smiley E, Bonadio J, Mooney DJ. DNA delivery from polymer matrices for tissue engineering. *Nat Biotechnol* 1999;17(6):551–4.
- [15] Jang JH, Rives CB, Shea LD. Plasmid delivery *in vivo* from porous tissue-engineering scaffolds: transgene expression and cellular transfection. *Mol Ther* 2005;12(3):475–83.
- [16] Riddle KW, Kong HJ, Leach JK, Fischbach C, Cheung C, Anseth KS, et al. Modifying the proliferative state of target cells to control DNA expression and identifying cell types transfected *in vivo*. *Mol Ther* 2007;15(2):361–8.
- [17] Blomeier H, Zhang X, Rives C, Brissova M, Hughes E, Baker M, et al. Polymer scaffolds as synthetic microenvironments for extrahepatic islet transplantation. *Transplantation* 2006;82(4):452–9.
- [18] Mooney DJ, Baldwin DF, Suh NP, Vacanti JP, Langer R. Novel approach to fabricate porous sponges of poly(D,L-lactic-co-glycolic acid) without the use of organic solvents. *Biomaterials* 1996;17(14):1417–22.
- [19] Harris LD, Kim BS, Mooney DJ. Open pore biodegradable matrices formed with gas foaming. *J Biomed Mater Res* 1998;42(3):396–402.
- [20] Heilmann C, von Samson P, Schlegel K, Attmann T, von Specht BU, Beyersdorf F, et al. Comparison of protein with DNA therapy for chronic myocardial ischemia using fibroblast growth factor-2. *Eur J Cardiothorac Surg* 2002;22(6):957–64.
- [21] Ando S, Putnam D, Pack DW, Langer R. PLGA microspheres containing plasmid DNA: preservation of supercoiled DNA via cryopreparation and carbohydrate stabilization. *J Pharm Sci* 1999;88(1):126–30.
- [22] Duvall CL, Taylor WR, Weiss D, Gulberg RE. Quantitative microcomputed tomography analysis of collateral vessel development after ischemic injury. *Am J Physiol Heart Circ Physiol* 2004;287(1):H302–10.
- [23] Hildebrand T, Rueggsegger P. A new method for the model-independent assessment of thickness in three-dimensional images. *J Microsc - Oxford* 1997;185:67–75.
- [24] Jang JH, Shea LD. Controllable delivery of non-viral DNA from porous scaffolds. *J Controlled Release* 2003;86(1):157–68.
- [25] Walter E, Moelling K, Pavlovic J, Merkle HP. Microencapsulation of DNA using poly(D,L-lactide-co-glycolide): stability issues and release characteristics. *J Controlled Release* 1999;61(3):361–74.
- [26] Charriere G, Cousin B, Arnaud E, Andre M, Bacou F, Penicaud L, et al. Pre-adipocyte conversion to macrophage. Evidence of plasticity. *J Biol Chem* 2003;278(11):9850–5.
- [27] Borden M, Attawia M, Khan Y, Laurencin CT. Tissue engineered microsphere-based matrices for bone repair: design and evaluation. *Biomaterials* 2002;23(2):551–9.
- [28] Schugens C, Grandfils C, Jerome R, Teyssie P, Delree P, Martin D, et al. Preparation of a macroporous biodegradable polylactide implant for neuronal transplantation. *J Biomed Mater Res* 1995;29(11):1349–62.
- [29] Taboas JM, Maddox RD, Krebsbach PH, Hollister SJ. Indirect solid free form fabrication of local and global porous, biomimetic and composite 3D polymer-ceramic scaffolds. *Biomaterials* 2003;24(1):181–94.
- [30] Liu Tsang V, Chen AA, Cho LM, Jadin KD, Sah RL, DeLong S, et al. Fabrication of 3D hepatic tissues by additive photopatterning of cellular hydrogels. *FASEB J* 2007;21(3):790–801.
- [31] Nof M, Shea LD. Drug-releasing scaffolds fabricated from drug-loaded microspheres. *J Biomed Mater Res* 2002;59(2):349–56.
- [32] Yew NS. Controlling the kinetics of transgene expression by plasmid design. *Adv Drug Deliv Rev* 2005;57(5):769–80.
- [33] Qin L, Ding Y, Pahud DR, Chang E, Imperiale MJ, Bromberg JS. Promoter attenuation in gene therapy: interferon-gamma and tumor necrosis factor-alpha inhibit transgene expression. *Hum Gene Ther* 1997;8(17):2019–29.
- [34] Zhang XY, Ni YS, Saifudeen Z, Asiedu CK, Supakar PC, Ehrlich M. Increasing binding of a transcription factor immediately downstream of the cap site of a cytomegalovirus gene represses expression. *Nucleic Acids Res* 1995;23(15):3026–33.
- [35] Prosch S, Stein J, Staak K, Liebenthal C, Volk HD, Kruger DH. Inactivation of the very strong HCMV immediate early promoter by DNA CpG methylation *In vitro*. *Biol Chem Hoppe-Seyler* 1996;377(3):195–201.
- [36] Loser P, Jennings GS, Strauss M, Sandig V. Reactivation of the previously silenced cytomegalovirus major immediate-early promoter in the mouse liver: involvement of NFkappaB. *J Virol* 1998;72(1):180–90.
- [37] Yew NS, Zhao H, Przybylska M, Wu IH, Tousignant JD, Scheule RK, et al. CpG-depleted plasmid DNA vectors with enhanced safety and long-term gene expression *in vivo*. *Mol Ther* 2002;5(6):731–8.
- [38] Hyde SC, Pringle IA, Abdullah S, Lawton AE, Davies LA, Varathalingam A, et al. CpG-free plasmids confer reduced inflammation and sustained pulmonary gene expression. *Nat Biotechnol* 2008;26(5):549–51.
- [39] Takakura Y, Takagi T, Hashiguchi M, Nishikawa M, Yamashita F, Doi T, et al. Characterization of plasmid DNA binding and uptake by peritoneal macrophages from class A scavenger receptor knockout mice. *Pharm Res* 1999;16(4):503–8.
- [40] Takagi T, Hashiguchi M, Mahato RI, Tokuda H, Takakura Y, Hashida M. Involvement of specific mechanism in plasmid DNA uptake by mouse peritoneal macrophages. *Biochem Biophys Res Commun* 1998;245(3):729–33.
- [41] Stacey KJ, Sweet MJ, Hume DA. Macrophages ingest and are activated by bacterial DNA. *J Immunol* 1996;157(5):2116–22.
- [42] Takahashi A, Palmer-Opolski M, Smith RC, Walsh K. Transgene delivery of plasmid DNA to smooth muscle cells and macrophages from a biostable polymer-coated stent. *Gene Ther* 2003;10(17):1471–8.
- [43] Fukuyama N, Tanaka E, Tabata Y, Fujikura H, Hagihara M, Sakamoto H, et al. Intravenous injection of phagocytes transfected *ex vivo* with FGF4 DNA/biodegradable gelatin complex promotes angiogenesis in a rat myocardial ischemia/reperfusion injury model. *Basic Res Cardiol* 2007;102(3):209–16.
- [44] Thomas ED, Ramberg RE, Sale GE, Sparkes RS, Golde DW. Direct evidence for a bone marrow origin of the alveolar macrophage in man. *Science* 1976;192(4243):1016–8.
- [45] De Laporte L, Cruz Rea J, Shea LD. Design of modular non-viral gene therapy vectors. *Biomaterials* 2006;27(7):947–54.
- [46] Anderson JM, Rodriguez A, Chang DT. Foreign body reaction to biomaterials. *Semin Immunol* 2008;20(2):86–100.